



# Interaction of benzopyranone derivatives and related compounds with human concentrative nucleoside transporters 1, 2 and 3 heterologously expressed in porcine PK15 nucleoside transporter deficient cells. Structure–activity relationships and determinants of transporter affinity and selectivity<sup>☆</sup>

Chunmei Wang, Surekha Pimple, John K. Buolamwini<sup>\*</sup>

Department of Pharmaceutical Sciences, College of Pharmacy, University of Tennessee Health Science Center, Memphis, TN, USA

## ARTICLE INFO

### Article history:

Received 26 June 2009

Received in revised form 26 August 2009

Accepted 28 August 2009

### Keywords:

Concentrative nucleoside transporters

Benzopyranone derivatives

CoMFA

CoMSIA

Structure–activity relationships

## ABSTRACT

Unlike the major equilibrative nucleoside transporters, there is a dearth of potent specific inhibitors of concentrative nucleoside transporters (CNTs). We investigated the interaction of benzopyranone derivatives and related compounds with human (h) CNTs in newly established PK15NTD transfectant cells stably expressing hCNT1 or hCNT2, and previously established PK15NTD/hCNT3 cells. Flavones exhibited the highest inhibitory activity against hCNT2 and hCNT3, whereas the most potent selective inhibitor of hCNT1 was a coumarin derivative. hCNT3 was the only transporter that exhibited moderate sensitivity to the chalcones tested. The most active compound was 6-hydroxy-7-methoxyflavone, which was hCNT3-specific with an  $IC_{50}$  of  $0.57 \pm 0.20 \mu\text{M}$ , and over 40-fold more potent than the standard CNT inhibitor, phloridzin ( $IC_{50}$  of  $25 \pm 3.5 \mu\text{M}$ ). The SAR (Structure–Activity Relationship) shows that high potency against all three hCNTs is conferred by the presence of hydroxyl substituents at both the 7- and 8-positions of flavones and isoflavones. CoMFA (Comparative Molecular Field Analysis) and CoMSIA (Comparative Molecular Similarity Indices Analysis) 3D-QSAR (three-Dimensional Quantitative Structure–Activity Relationship) modeling indicated that electrostatic and hydrophobic properties were the most influential for interactions between the flavonoids and hCNT1, while electrostatic, hydrophobic and hydrogen bond donor properties were predominate for interactions with hCNT2 and hCNT3. The 3D-QSAR results also suggested possible commonalities in hydrogen bonding interactions of flavonoids and nucleosides, suggesting similarities between the hCNT-binding sites of the two classes of compounds. We report the most potent and selective non-nucleoside CNT inhibitors to date; which may serve as research tools and/or leads for further inhibitor development.

© 2009 Elsevier Inc. All rights reserved.

## 1. Introduction

Physiological nucleosides and many nucleoside drugs are hydrophilic molecules that do not readily cross biological membranes, and are translocated across them by specialized transmembrane proteins termed nucleoside transporters [1,2]. Nucleoside transporters are important for the salvage and disposal of nucleosides, and the modulation of the local concentrations of signaling nucleosides such as adenosine [2–4]. They are also

pharmacologically important for the absorption of nucleoside drugs [5–7]. Nucleoside transporters are divided into two major families: the SLC29 equilibrative nucleoside transporter (ENT) family [8] and the SLC28 concentrative nucleoside transporter (CNT) family [9]. Concentrative nucleoside transport is a high-affinity uphill process unlike equilibrative nucleoside transport which is a  $\text{Na}^+$ -independent facilitated diffusion process. Six concentrative nucleoside transporters have been identified but only the three major isoforms, CNT1 (SLC28A1), CNT2 (SLC28A2) and CNT3 (SLC28A3) have been cloned [10–15]. They are predicted to be 13 (or possibly 15) transmembrane (TM) helical domain proteins [10,16]. Unlike ENTs, which are generally broad substrate specificity nucleoside transporters, CNTs have marked substrate specificity differences. Thus, whereas CNT1 and CNT2 generally transport pyrimidine and purine nucleosides, respectively; CNT3 transports both classes of nucleosides equally well. hCNT1 and hCNT2 have a  $\text{Na}^+$ -nucleoside coupling ratio of 1:1, whereas for

<sup>☆</sup> This study was supported in part by the National Cancer Institute [Grant CA-101856].

<sup>\*</sup> Corresponding author at: Department Pharmaceutical Sciences, College of Pharmacy, University of Tennessee Health Science Center, 847 Monroe Avenue, Suite 327, Memphis, TN 38163, USA. Tel.: +1 901 448 7533; fax: +1 901 448 6828.

E-mail address: [jbuolamwini@utmem.edu](mailto:jbuolamwini@utmem.edu) (J.K. Buolamwini).

hCNT3 the Na<sup>+</sup>-nucleoside coupling ratio is 2:1 [15], which implies that hCNT3 can concentrate nucleosides 10-fold higher than either hCNT1 or hCNT2. hCNT3 can also function as a H<sup>+</sup>-nucleoside cotransporter, whereas hCNT1/2 cannot. This capability of hCNT3 is said to be relevant to its putative involvement in renal reabsorption of nucleosides and nucleoside drugs [17].

Pathological overexpression of hCNTs appears to occur in some cancers and can adversely affect antimetabolite chemotherapy. For example overexpression of hCNT1 was shown to correlate with relapse and reduced survival of breast cancer patients treated with combination therapy containing 5-fluorouracil; and the overexpression of hCNT3 in CLL cells has been shown to correlate with a lower response rate to fludarabine [18]. On the other hand, expression of a particular hCNT transporter may be required for successful therapy with nucleoside-based anticancer drugs [19].

While many potent and specific inhibitors of ENTs have been identified, such inhibitors are acutely lacking for CNTs [20], thus hindering studies of their physiological functions and targeting for therapeutic purposes. Benzopyranone derivatives such as flavonoids and related compounds occur widely in nature, and are found in fruits and vegetables, and have been shown to inhibit cell membrane solute transporters like glucose transporters [21]. We therefore investigated the interaction of these compounds with hCNTs with the aim of identifying novel selective CNT inhibitors. We report here the stable expression of hCNT1 and hCNT2 in PK15NTD cells created by Ward et al. [22], and their use together with previously established PK15 cells expressing hCNT3, to identify novel potent selective inhibitors of each of the three CNTs. Quantitative structure–activity relationship (QSAR) modeling was used to rationalize the structural determinants of inhibitory potency and transporter selectivity and to gain insights for inhibitor design.

## 2. Materials and methods

### 2.1. Materials

PCR-ready human kidney cDNA was obtained from Ambion (Austin, TX). pCMV-3tag-1 mammalian expression vector and pfu DNA polymerase were purchased from Stratagene (La Jolla, CA). Restriction enzymes were obtained from New England Biolabs (Ipswich, MA). The transfection reagent, Lipofectamine 2000, was purchased from Invitrogen (Carlsbad, CA). FLAG antibody was obtained from Sigma–Aldrich (St. Louis, MO), and species-specific horseradish-peroxidase secondary antibody was from Santa Cruz (Santa Cruz, CA). ECL was purchased from Amersham Biosciences (Piscataway, NJ). [5-<sup>3</sup>H]Uridine (1 mCi/ml, 27.0 Ci/mmol) was supplied by GE Healthcare (Piscataway, NJ). All reagents were of either molecular biology or cell culture-tested grade.

### 2.2. Chemicals

Phloridzin, NBMPR, compounds **78**, **79** and **80**, as well as all non-radioactive nucleosides were purchased from Sigma–Aldrich (St. Louis, MO). Compounds **48**, **75** and **88** were purchased from Alfa Aesar (Ward Hill, MA), compound **49** from TimTec (Newark, DE), compound **74** from ChemBridge (San Diego, CA), compounds **81** and **82** from Princeton Gold Collection (Monmouth Junction, NJ), compound **83** from LaboTest (Niederschona, Germany), compound **87** from TCI (Portland, OR); and the rest of the compounds were purchased from Indofine Chemical Company (Hillsborough, NJ).

### 2.3. Cell culture

Porcine kidney tubular epithelium nucleoside transporter deficient cells and PK15 cells stably expressing hCNT3 were kindly

donated by Dr. Chung-Ming Tse (Johns Hopkins University, Baltimore, MD). Cells were maintained in Eagle's minimal essential medium/Earle's Balanced Salt Solution with 0.1 mM nonessential amino acids, 1 mM sodium pyruvate (ATCC, Manassas, VA) and 10% fetal bovine serum (Invitrogen, Grand Island, NY) at 37 °C in a humidified atmosphere of a mixture of 5% CO<sub>2</sub> and 95% air.

### 2.4. Cloning of hCNT1 and hCNT2

Full-length hCNT1 and hCNT2 cDNA (GenBank accession nos. HSU62966 and BC112047) were obtained by polymerase chain reaction from PCR-ready human kidney cDNA. PCR amplification was performed using the following primers flanking the hCNT1 and hCNT2 open reading frame (restriction sites underlined): sense-EcoRV-hCNT1: 5'-AGC GATATCTGG GAC ATG GAG AAC GAC-3', antisense-Sall-hCNT1: 5'-TTA GTC GAC TGT TCT GTC CTC ACT GTG CAC-3'; sense-BamHI-hCNT2: 5'-AGG TTA GGA TCC GAG ATG GAG AAA GCA AGT G-3', antisense-XhoI-hCNT2: 5'-TCA GAA CTC GAG CTT AGG CAC AGA CGG TAT TG-3'. The PCR sample (50 µl) contained 2 µl of cDNA template, 2.5U of pfu DNA polymerase, 0.2 mM of dNTP and 25 pmol of both sense and antisense primers. The first PCR amplification cycle was performed at 95 °C for 5 min; this was followed by 29 cycles at 94 °C for 45 s, 52 °C for 45 s and 72 °C for 4 min; and a last PCR cycle at 72 °C for 10 min to generate products of approximately 2 kb. The hCNT1 and hCNT2 PCR products were cloned into the mammalian expression vector pCMV-3flag-1A. Positive clones were confirmed by colony PCR and restriction analysis, and were subjected to DNA sequencing (Molecular Resources Center, University of Tennessee Health Science Center, Memphis, TN).

### 2.5. Selection of PK15 cells stably expressing recombinant hCNT1 and hCNT2

To generate hCNT1 and hCNT2 stable transfectants, 6 × 10<sup>5</sup> cells/well were seeded in six-well plates in modified minimal Eagle's medium one day before transfection, which allowed them to reach about 95% confluence. The pCMV-3flag/hCNT1 and pCMV-3flag/hCNT2 expression constructs were transfected into PK15NTD cells using Lipofectamine 2000 according to the manufacturer's instructions (Invitrogen, Carlsbad, CA). Cells were transferred into a 100 mm dish at 1:10 dilution in growth medium containing G418 (Invitrogen, Grand Island, NY) 48 h after transfection. After selection for three weeks, cell colonies were picked up using cloning cylinders and screened by the successful reconstitution of Na<sup>+</sup>-dependent [<sup>3</sup>H]uridine uptake.

### 2.6. Membrane preparation and western blot analysis

Crude membranes were purified from vector, hCNT1 and hCNT2 transfected cells by lysis and sonication in buffer without Triton X-100 containing 25 mM Tris–HCl, 150 mM NaCl, 2 mM MgCl<sub>2</sub>, 1 mM EGTA and 1 mM EDTA (pH 7.4). The cell lysate was then centrifuged for 1 h at 100,000 × g. The pellet was resuspended and sonicated in buffer containing 1% Triton X-100 in addition to the above components. The resulting supernatant was collected, followed by centrifugation for 15 min at 14,200 × g. SDS-PAGE was performed, after which the proteins were transferred onto polyvinylidene difluoride membranes (Bio-Rad, Hercules, CA). After blocking in TBST (0.1% Tween 20, Tris-buffered saline) containing 5% non-fat dry milk, membranes were incubated in blocking buffer containing mouse FLAG monoclonal antibody overnight at 4 °C. The membranes were then washed three times with TBST, incubated with TBST containing anti-mouse horseradish-peroxidase secondary antibody, washed with TBST and detected by enhanced chemiluminescence.

## 2.7. [<sup>3</sup>H]uridine uptake and inhibition assay

All uptake assays were carried out in triplicate. Cells were seeded at  $3 \times 10^4$ /well densities in 48-well plates two days before the experiments. To conduct the uptake assay, cells were washed twice with sodium-free buffer (choline chloride 120 mM, Tris–HCl 20 mM, K<sub>2</sub>HPO<sub>4</sub> 3 mM, glucose 10 mM, MgCl<sub>2</sub> 1 mM, CaCl<sub>2</sub> 1 mM, pH7.4) and incubated with sodium-free buffer or sodium-containing buffer (NaCl 120 mM, Tris–HCl 20 mM, K<sub>2</sub>HPO<sub>4</sub> 3 mM, glucose 10 mM, MgCl<sub>2</sub> 1 mM, CaCl<sub>2</sub> 1 mM, pH7.4) for 30 min. Then 1 μM of [<sup>3</sup>H]uridine in sodium-free or sodium-containing buffer was added to each well and incubated for 2 min. For inhibition assay, the cells were preincubated with sodium-containing buffer containing test compound for 15 min before addition of 0.2 μM [<sup>3</sup>H]uridine solution, and incubation for 2 min. Uptake was terminated by rapidly aspirating the incubation mixture and washing cells three times with ice-cold PBS. The cells were solubilized overnight in 300 μl of 5% Triton X-100 and 200 μl of cell lysate was counted using a scintillation counter. Protein concentration in the cell lysate was determined using the BCA protein assay kit (Pierce, Rockford, IL).

## 2.8. Kinetic analysis

Time-course uptake experiments were conducted by incubating cells with [<sup>3</sup>H]uridine for variable time in sodium-free or sodium-containing buffer. The uptake rate was obtained by [<sup>3</sup>H]uridine uptake for 10, 20, 30 and 60 s in sodium-containing buffer excluding the diffusion in the absence of Na<sup>+</sup>.  $K_m$  and  $v_{max}$  values for uridine uptake were determined by fitting the data to the Michaelis–Menten equation (Eq. (1)).

$$\frac{1}{v} = \frac{K_m}{v_{max}[S]} + \frac{1}{v_{max}} \quad (1)$$

where  $v$  is initial uptake rate,  $K_m$  is the Michaelis–Menten constant,  $v_{max}$  is the maximum rate, and  $[S]$  is the substrate concentration.

## 2.9. Data analysis

GraphPad Prism 5.0 was used for graphing and statistical analysis (version 5.0, GraphPad, San Diego, CA). The concentration of test compounds that caused 50% inhibition of [<sup>3</sup>H]uridine uptake was calculated using the nonlinear regression fitting method in the Prism program. Nucleoside uptake data are expressed as means ± S.E. for triplicate estimates of individual experiments ( $n = 3$ ). Statistical significance was determined by Student's  $t$ -test analysis, and a  $P < 0.05$  was considered statistically significant.

## 2.10. CoMFA and CoMSIA 3D-QSAR Modeling

3D-QSAR modeling was carried out using CoMFA [23] and CoMSIA [24] methods. IC<sub>50</sub> values were converted to  $K_i$  values and transformed into  $pK_i$  ( $-\log_{10} K_i$ ) values, which were then used as dependent variable in CoMFA and CoMSIA models. Three-dimensional structure building and all modeling operations were performed using the SYBYL 7.3 molecular modeling program (Tripos Associates Inc., 2006) on a Silicon Graphics Octane workstation (Silicon graphics, San Diego, CA). Energy minimization was performed using the Tripos force field with a distance dependent dielectric and the BFGS algorithm, with a convergence criterion of 0.01 kcal/(mole × Å). Structural geometries were further optimized with the AM1 Hamiltonian in the MOPAC semi-empirical program in SYBYL, which was also used to assign partial atomic charges. The compounds were aligned by the automatic

alignment function in SYBYL, using the minimized energy conformation of compound **49**, the compound with high potency against all the three hCNTs as the alignment template. CoMFA and CoMSIA descriptor fields were generated by first placing the aligned molecules in a three-dimensional cubic lattice with a grid spacing of 2 Å and extending 4 Å units beyond the aligned molecules in all directions; and then were calculating steric (Lennard–Jones 6–12 potential) and electrostatic (coulombic) energy fields using an sp<sup>3</sup> carbon probe atom with a van der Waals radius of 1.52 Å and a charge of +1.0. An energy cutoff at 30 kcal/mol was applied, and fields were scaled by the CoMFA-STD method.

CoMSIA similarity index descriptors were calculated using a similar lattice box as the one employed in the CoMFA descriptor calculations, according to the procedure of Klebe et al. [24]. CoMSIA descriptors, namely, steric, electrostatic, hydrophobic, hydrogen bond donor, and hydrogen bond acceptor, were generated using a sp<sup>3</sup> carbon probe atom with +1.0 charge and a van der Waals radius of 1.4 Å. Similarity indices ( $A_{F,k}$ ) between a molecule  $j$  and atom  $i$  at a grid point were calculated using Eq. (2).

$$A_{F,k}^q(j) = -\sum \omega_{probe,k} \omega_{ik} e^{-\alpha i q^2} \quad (2)$$

The steric, electrostatic, hydrophobic, hydrogen bond donor or hydrogen bond acceptor descriptor  $k$  of atom  $i$  is  $\omega_{ik}$ , while the corresponding descriptor of the probe atom is  $\omega_{probe}$ . A Gaussian-type distance dependence was used between the grid point  $q$  and each atom  $i$  in the molecule with an attenuation factor ( $\alpha$ ) of 0.3. Steric indices were derived from atomic radii, electrostatic descriptors from atomic partial charges, hydrophobic fields were derived from atom-based parameters, and hydrogen bond donor and acceptor indices were derived from experimental data.

Using CoMFA and CoMSIA descriptors as independent variables and  $pK_i$  values as dependent variable, partial least squares (PLS) regression analyses were carried out as implemented in the QSAR module of the SYBYL package. Leave-one-out (LOO) cross-validation was used to evaluate the predictive ability. The cross-validated coefficient,  $q^2$ , was calculated using Eq. (3).

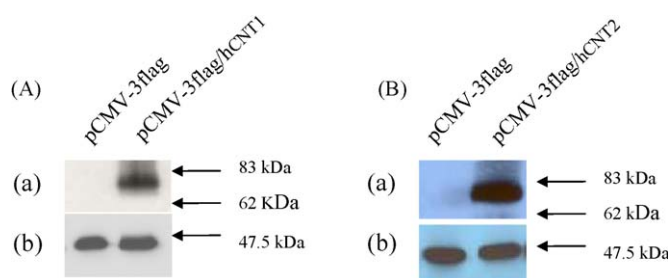
$$q^2 = 1 - \frac{\sum (Y_{predicted} - Y_{actual})^2}{\sum (Y_{observed} - Y_{mean})^2} \quad (3)$$

where  $Y_{predicted}$ ,  $Y_{actual}$ , and  $Y_{mean}$  are predicted, actual and mean values of the dependent property ( $pK_i$ ), respectively; and  $\sum (Y_{predicted} - Y_{actual})^2$  is the predictive sum of squares (PRESS). The optimum number of components used to set up the final regression models was that which afforded the lowest PRESS value. The conventional correlation coefficient ( $r^2$ ) and its standard error of estimate ( $s$ ) were also calculated. The robustness of the models was tested by rigorous methods of group-cross-validation and bootstrapping. To rule out chance correlations, PLS regression analyses were also carried out using scrambled activity data (randomization). CoMFA and CoMSIA contour maps were generated by interpolation of the products of the PLS coefficients and the standard deviations of the corresponding CoMFA and CoMSIA descriptor.

## 3. Results and discussion

### 3.1. Expression of recombinant hCNT1 and hCNT2 in PK15NTD cells

The hCNT3 transporter has been stably expressed in the attached cell line PK15NTD [25], and has been used by us in the discovery of new hCNT3 inhibitors [26]. However, no such attached cell line system expressing either hCNT1 or hCNT2 was available to us. Thus, to embark on a program of identifying potent and specific inhibitors for individual CNTs, we cloned and stably expressed



**Fig. 1.** Immunoblotting detection of recombinant hCNT1 and hCNT2 expressed in PK15NTD cells. PK15NTD cells were transfected with pCMV-3flag vector, pCMV-3flag/hCNT1 (A(a)) or pCMV-3flag/hCNT2 (B(a)). Cell membrane fractions were analyzed by Western blotting using FLAG antibody. The blots were reprobed for  $\beta$ -actin for normalization (A(b) and B(b)).

hCNT1 and hCNT2 transporters individually in the PK15NTD cells. Our cDNA clones had an identical predicted protein sequences with the 650-residue hCNT1 or 658-residue hCNT2 protein in the GenBank. The recombinant hCNT1 and hCNT2 were successfully transfected and expressed in nucleoside transport deficient PK15NTD cells to create new flag-tagged hCNT1 and hCNT2 mammalian expression systems. Western blotting using FLAG antibody was used for verification. A protein product of  $\sim 75$  kDa was detected in the cells with recombinant hCNT1 and hCNT2, which was absent in cells transfected with the empty vector control as shown in Fig. 1.

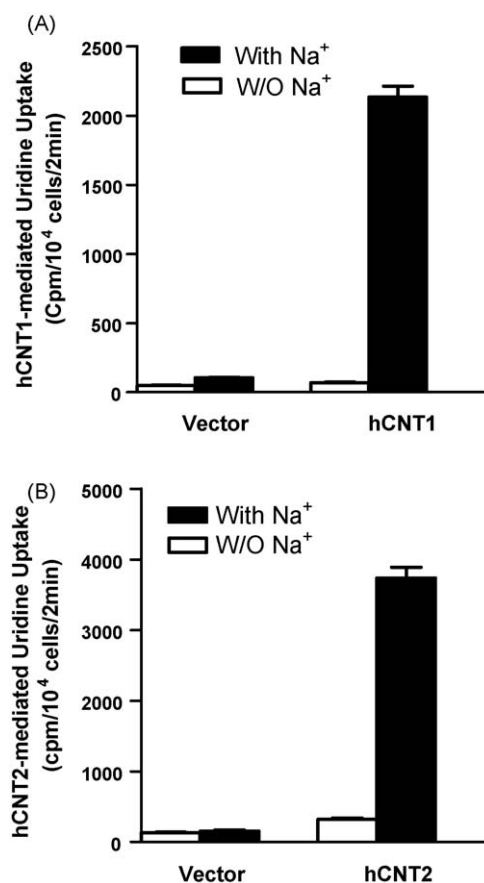
### 3.2. Uridine transport by hCNT1 or hCNT2 produced in PK15NTD cells

To determine the nucleoside transport function of the expressed hCNT1 and hCNT2 proteins, we performed [ $^3$ H]uridine uptake experiments under sodium and sodium-free conditions. Transient transfection of pCMV-3flag/hCNT1 into PK15NTD cells resulted in about 20-fold higher [ $^3$ H]uridine uptake than transfection with vector, and about 30-fold higher uptake in the presence of  $\text{Na}^+$  ion than in the absence of  $\text{Na}^+$  ion (Fig. 2A). Similarly, there was approximately 24-fold as much uptake in pCMV-3flag/hCNT2 transfected cells as in vector-transfected cells, and 10-fold as much uptake in the presence of  $\text{Na}^+$  ion as in its absence (Fig. 2B).

The time-course of  $1 \mu\text{M}$  [ $^3$ H]uridine uptake by PK15/hCNT2 cells was linear over the time span examined in the presence of  $\text{Na}^+$ . The uptake of [ $^3$ H]uridine in PK15/hCNT1 cells also increased over time, but the time-course was not linear. There was again not much uptake in the absence of  $\text{Na}^+$  for both hCNT1 and hCNT2 (Fig. 3). These data confirmed the expression of functional hCNT1 and hCNT2 in the plasma membranes of the PK15NTD cells. The kinetic parameters,  $K_m$  and  $v_{max}$ , for uridine uptake were  $6.8 \pm 2.6 \mu\text{M}$  and  $111.6 \pm 23.7 \text{ pmol/mg protein/min}$ , and  $5.4 \pm 3.1 \mu\text{M}$  and  $93.2 \pm 8.4 \text{ pmol/mg protein/min}$  for hCNT1 and hCNT2, respectively. The data show that hCNT1 and hCNT2 transporters expressed in PK15 cells have a higher affinity for uridine than those expressed in *Xenopus laevis* oocytes [12,14,27], yeast [28] or leukemia cells [29], which may be due to differences in post-translational modifications and/or differences in membrane environments [30].

### 3.3. Interaction of Nucleosides and NT Inhibitors with recombinant hCNT1 and hCNT2 stably expressed in PK15 cells

The hCNT1 transporter generally transports pyrimidine nucleosides and adenosine, whereas hCNT2 prefers purine nucleosides and uridine. In addition to demonstrating that both hCNT1 and hCNT2 transport uridine quite well, we also tested their substrate selectivity by measuring the inhibitory activities of various natural



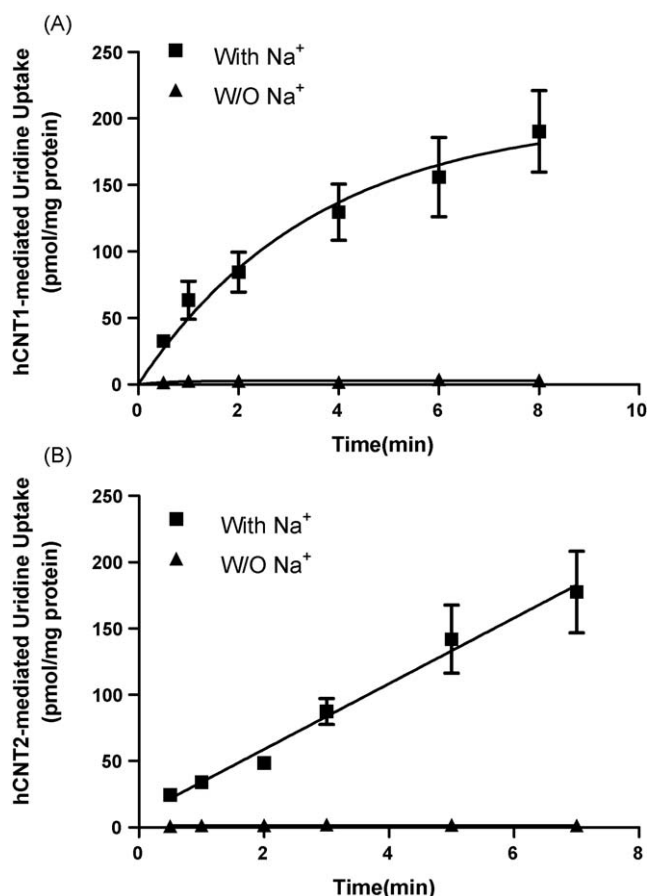
**Fig. 2.** [ $^3$ H]Uridine uptake by PK15NTD transiently transfected with recombinant hCNT1 and hCNT2. Cells were incubated with  $0.2 \mu\text{M}$  [ $^3$ H]uridine in either sodium-containing or sodium-free buffer for 2 min. PK15NTD cells transfected with empty vector were used as control.

purine and pyrimidine nucleosides. As shown in Fig. 4, uridine uptake in PK15/hCNT1 cells was inhibited by pyrimidine nucleosides and adenosine but not by purine nucleosides; whereas hCNT2-mediated uridine uptake was inhibited by purine nucleosides but not by cytidine or thymidine, showing functional characteristics attributable to hCNT1 and hCNT2, respectively [14]. Further, we tested the inhibitory activities of nitrobenzylmercaptapurine riboside (NBMPR) and phloridzin. There was no significant inhibition of hCNT2, and low inhibition of hCNT1 by  $10 \mu\text{M}$  NBMPR (a specific ENT1 inhibitor), whereas phloridzin, a standard CNT inhibitor, exhibited marked inhibitory activity against hCNT1 at  $250 \mu\text{M}$  and against hCNT2 at  $100 \mu\text{M}$ , consistent with the inhibitor interaction profiles of hCNT1 and hCNT2 (Fig. 4). These results also confirmed the identities of the two recombinant transporters.

### 3.4. Interaction of benzopyranone derivatives and related compounds with recombinant hCNT1, hCNT2 and hCNT3 transporters

Our objective in embarking on this work was to identify much-needed potent and specific inhibitors of concentrative nucleoside transporters. Thus, we tested the inhibition of [ $^3$ H]uridine transport in our newly created PK15/hCNT1 and PK15/hCNT2 cells (stably expressing the transporters), and PK15 cells expressing hCNT3, by a series of benzopyranone derivatives including flavones, isoflavones and coumarins, as well as chalcones and related compounds (Table 1). Chalcones were included because they are related to the aglycone of the standard CNT inhibitor phloridzin [10,25], which is a dihydrochalcone glucoside, and we

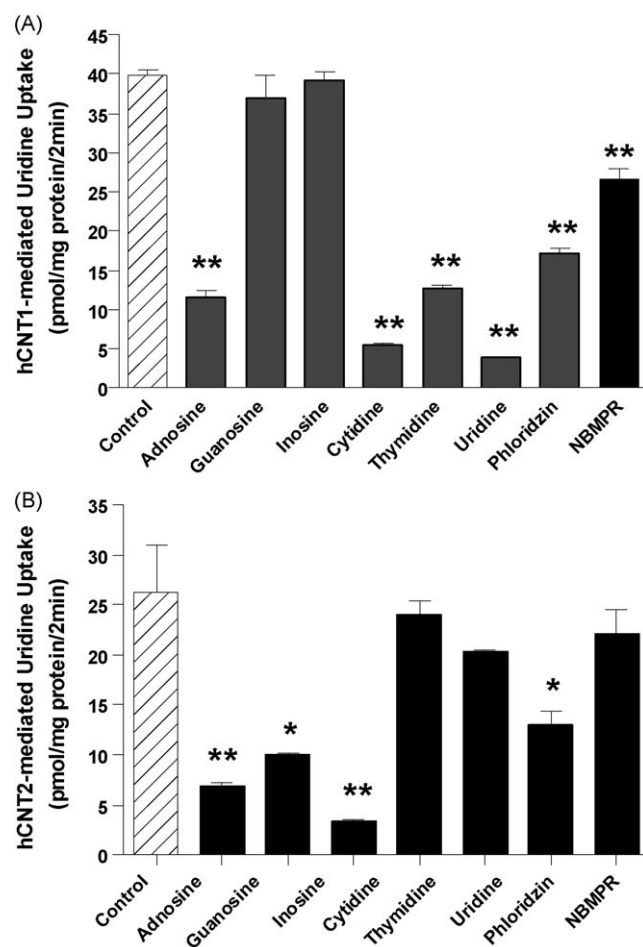




**Fig. 3.** Time-course of [<sup>3</sup>H]uridine uptake in hCNT1 and hCNT2 stable transfectant cells. The uptake of 1  $\mu$ M [<sup>3</sup>H]uridine was measured in the presence or the absence of 120 mM NaCl at the time points shown. Data points are the mean  $\pm$  S.E.M. ( $n = 3$ ).

have recently shown that phloretin, the aglycone of phloridzin is an inhibitor of hCNT3 [26]. The compounds were first screened at 10  $\mu$ M (Fig. 5), and for those that showed significant inhibitory activity at that concentration, dose-response assays were carried out to derive  $IC_{50}$  values (Table 2). Dose-response curves for the potent and selective compounds for each hCNT are shown in Fig. 6. The compounds exhibited wide ranging inhibitory activities and selectivities such that while most were inactive ( $<30\%$  inhibition) against hCNT1 and hCNT2, most were active ( $\geq 30\%$  inhibition) against hCNT3 (Fig. 5). The compounds that were followed up for  $IC_{50}$  determinations, exhibited hCNT inhibitory  $IC_{50}$  values in the range 0.57–231  $\mu$ M (Table 2), with most of those compounds exhibiting much higher potencies than the standard inhibitor phloridzin.

Interestingly, hCNT1, which was not as sensitive to the flavones as either hCNT2 or hCNT3, was the only one that was potently inhibited by the coumarin derivative 7-hydroxy-3-(4'-methoxyphenyl)coumarin (compound **89**,  $IC_{50} = 4.44 \mu$ M). Although it is premature to single out the coumarin class as potential specific inhibitors of hCNT1, compound **89** might serve as a lead compound for the design of much-needed potent hCNT1 inhibitors. Compounds **13**, **34**, **49**, **50**, **51**, **57** and **85** inhibited hCNT2, while compounds **11**, **12**, **13**, **34**, **39**, **49**, **50**, **51**, **57**, **72**, **74**, **83**, and **84** inhibited hCNT3 with  $IC_{50}$ s less than 10  $\mu$ M (Table 2). The most potent inhibitor of hCNT2 was the flavone derivative 3',7,8-trihydroxyflavone (compound **49**,  $IC_{50} = 1.66 \mu$ M). This compound was also the most potent flavone inhibitor of hCNT1 ( $IC_{50} = 11.75 \mu$ M), possibly pointing to a similarity between the flavone-binding sites of these two transporters. The most potent



**Fig. 4.** Nucleoside specificity and inhibitor profiles of hCNT1 and hCNT2 stably expressed in PK15NTD cells. Uptake of 1  $\mu$ M [<sup>3</sup>H]uridine for 2 min was measured in PK15/hCNT1 (A) and PK15/hCNT2 (B) cells in the absence (control) or presence of 100  $\mu$ M non-radioactive nucleoside, 10  $\mu$ M NBMPR or phloridzin (250  $\mu$ M for hCNT1; 100  $\mu$ M for hCNT2) for 15 min. Data points are the mean  $\pm$  S.E.M. ( $n = 3$ ). \* $P < 0.05$ , \*\* $P < 0.01$  compared with transport in control.

and selective hCNT3 inhibitor was the flavone derivative 6-hydroxy-7-methoxyflavone (compound **39**,  $IC_{50} = 0.57 \mu$ M), an activity much higher than that of phloridzin ( $IC_{50} = 25 \mu$ M). In fact, this compound is even more active than the most potent phloridzin analog we recently reported, which exhibited hCNT3 inhibitory  $IC_{50}$  of 2.88  $\mu$ M [26]. Another potent inhibitor of hCNT3 that stands out is the flavone derivative compound **50** ( $IC_{50} = 0.68 \mu$ M), which also potently inhibited hCNT2 ( $IC_{50} = 5.25 \mu$ M) but only moderately inhibited hCNT1 ( $IC_{50} = 29.39 \mu$ M). Compounds **13**, **49**, **50**, **51** and **57** are related compounds, all of which contain the high potency-conferring 7,8-dihydroxy substitution but differ only in the hydroxylation pattern of the 2-position phenyl ring. The lack of a hydroxyl group on this phenyl ring (compound **13**) is more detrimental to activity against hCNT1 than the other two transporters; and monohydroxylation at the 2'-position was optimal for hCNT1 inhibition (compound **57**). This suggests that there might be a favorable H-bond interaction at that region on hCNT1. With hCNT2 and hCNT3, it was rather the presence of a hydroxyl group at the 3'-position or 4'-position, respectively that gave the highest activity. Monohydroxylation at the 2'-position significantly decreased hCNT3 inhibition but not hCNT1 or hCNT2. These data are interesting in that although the high potency of these compounds against all three hCNTs suggests similarities in the flavone-binding sites of the three transporters, the site

**Table 1**

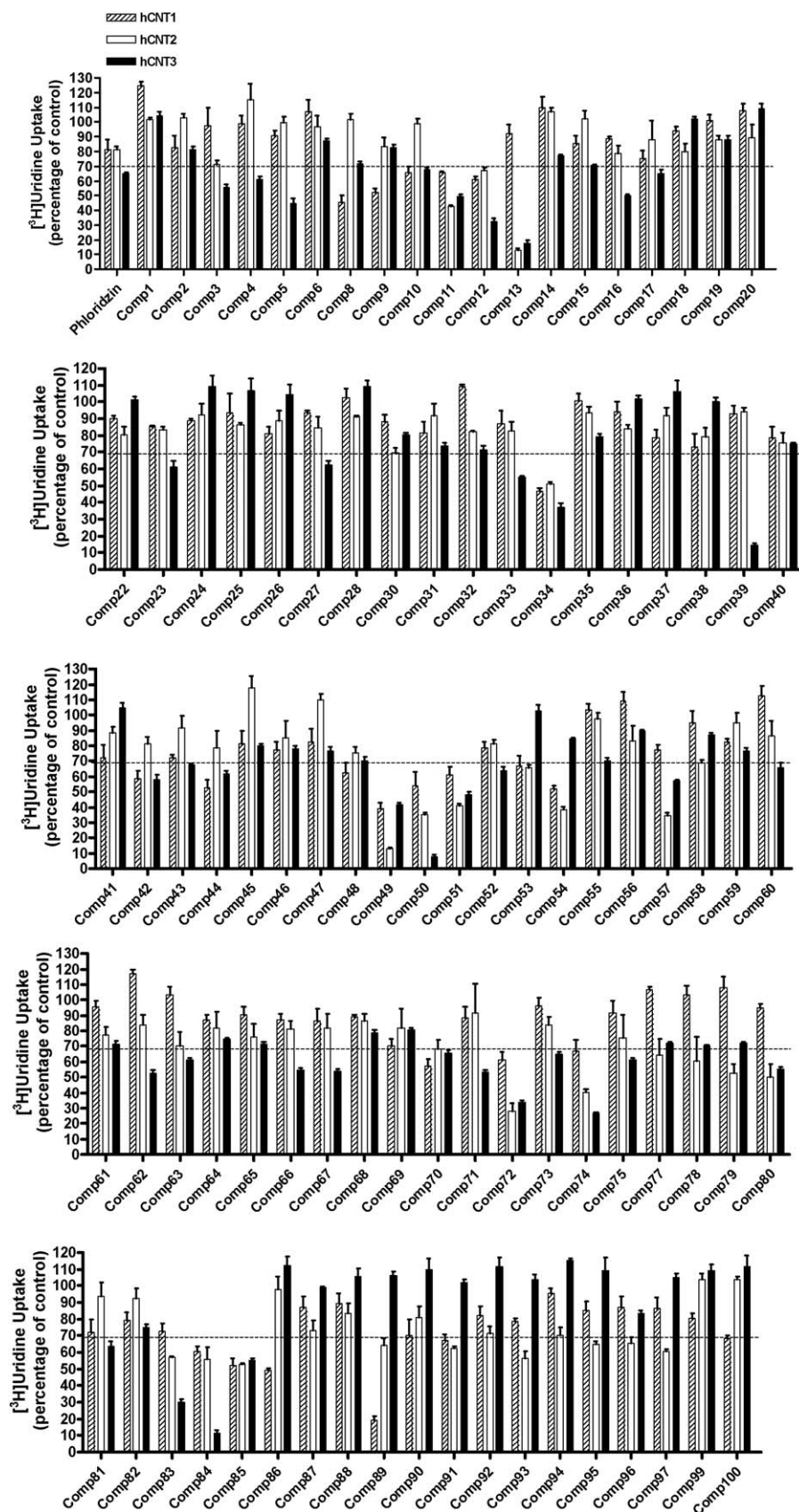
Benzopyrone derivatives and related compounds tested for hCNT1, hCNT2 and hCNT3 transporter inhibitory activity.

| Compd. no. | Name  | Compd. no. | Name   |
|------------|---|------------|--|
| 1          | 4'-Bromo-6-chloro-7-methylflavone                       | 52         | 5,6-Dihydroxyflavone   |
| 2          | 3,4'-Dihydroxyflavone                                   | 53         | 5,7-Dihydroxyflavone   |
| 3          | 3',4'-Dihydroxyflavone                                  | 54         | 3',4'-Dihydroxy- $\alpha$ -naphthoflavone                    |
| 4          | 3,5-Dihydroxyflavone                                    | 55         | 7,8-Dimethoxyflavone   |
| 5          | 3,6-Dihydroxyflavone                                    | 56         | 8-Hydroxy-7-methoxyflavone                                   |
| 6          | 3,7-Dihydroxyflavone                                    | 57         | 7,8,2'-Trihydroxyflavone                                     |
| 8          | 6,4'-Dihydroxyflavone                                   | 58         | 4'-Chloro-7-hydroxy-8-methylisoflavone                       |
| 9          | 6,7-Dihydroxyflavone                                    | 59         | 7-Hydroxy-8-methylisoflavone                                 |
| 10         | 7,2'-Dihydroxyflavone                                   | 60         | 5,6-Benzoflavone   |
| 11         | 7, 3'-Dihydroxyflavone                                  | 61         | 7,8-Benzoflavone   |
| 12         | 7,4'-Dihydroxyflavone                                   | 62         | 3',4'-Dihydroxy- $\beta$ -naphthoflavone                     |
| 13         | 7,8-Dihydroxyflavone                                    | 63         | 3',4'-Dimethoxy- $\alpha$ -naphthoflavone                    |
| 14         | 5,4'-Dihydroxy-7-methoxyflavone                         | 64         | 2'-Hydroxy- $\alpha$ -naphthoflavone                         |
| 15         | 5,6-Dihydroxy-7-methoxyflavone                          | 65         | 2'-Hydroxy- $\beta$ -naphthoflavone                          |
| 16         | 3,7-Dihydroxy-3',4',5'-trimethoxyflavone                | 66         | 3'-Hydroxy- $\alpha$ -naphthoflavone                         |
| 17         | 5,3'-Dihydroxy-6,7,4'-trimethoxyflavone                 | 67         | 3'-Hydroxy- $\beta$ -naphthoflavone                          |
| 18         | 2',3'-Dimethoxyflavone                                  | 68         | 4'-Hydroxy- $\alpha$ -naphthoflavone                         |
| 19         | 3,4'-Dimethoxyflavone                                   | 69         | 4'-Hydroxy- $\beta$ -naphthoflavone                          |
| 20         | 3',4'-Dimethoxyflavone                                  | 70         | 3-Methoxy furano-2,3,7,8-flavone (Karanjin)                  |
| 22         | 6,7-Dimethoxyflavone                                    | 71         | 4'-Methoxy- $\alpha$ -naphthoflavone                         |
| 23         | 3',4'-Dimethoxyflavonol                                 | 72         | 5,7,3',4',5'-Pentahydroxyflavone                             |
| 24         | 2',3'-Dimethoxy-3-hydroxyflavone                        | 73         | 7,4'-Dihydroxy-8-C-glucosylisoflavone (Puerarin)             |
| 25         | 2',4'-Dimethoxy-3-hydroxyflavone                        | 74         | 7,8-Dihydroxy-3-(1-phenyl-1H-pyrazol-4-yl)-4H-chromen-4-one  |
| 26         | 6,2'-Dimethoxy-3-hydroxyflavone                         | 75         | Flavone  |
| 27         | 6,3'-Dimethoxy-3-hydroxyflavone                         | 77         | 6,8-Dichloroflavone  |
| 28         | 6,4'-Dimethoxy-3-hydroxyflavone                         | 78         | 3-(4-Chlorophenoxy-7,8-dihydroxy)-4H-chromen-4-one           |
| 30         | 7,3'-Dimethoxy-3-hydroxyflavone                         | 79         | 3-(4-Fluorophenoxy-7,8-dihydroxy)-4H-chromen-4-one           |
| 31         | 2',4'-Dimethoxy-3-hydroxy-6-methylflavone               | 80         | 7,8-Dihydroxy-2-methyl-3-phenyl-4H-chromen-4-one             |
| 32         | 3',4'-Dimethoxy-3-hydroxy-6-methylflavone               | 81         | 4H-1-benzopyran-4-one,6,7-dihydroxy-3-phenyl-                |
| 33         | 6,7-Dimethoxy-5,3',4'-trihydroxyflavone                 | 82         | 4H-1-benzopyran-4-one,7,8-dihydroxy-3-phenyl-                |
| 34         | 3,7,3',4'-tetrahydroxyflavone (Fisetin)                 | 83         | 4H-1-benzopyran-4-one,7,8-dihydroxy-3-(4-methyl-2-thiazoyl)- |
| 35         | 5-Hydroxy-6,7,8,3',4',5'-hexamethoxyflavone (Gardenin)  | 84         | 3,7,3',4',5'-Pentahydroxyflavone (Robinetin)                 |
| 36         | 3,5,7,8,3',4'-Hexahydroxyflavone (Gossypetin)           | 85         | 7,3',4',5'-Tetrahydroxyflavone                               |
| 37         | 3,5,7,8,3',4'-Hexahydroxyflavone-8-glucoside (Gossypin) | 86         | 2,3,4,3',4',5'-Hexahydrobenzophenone                         |
| 38         | 5,6,7,3',4',5'-Hexamethoxyflavone                       | 87         | Dibromopyrogallolsulfonphthaleine (Bromopyrogallol red)      |
| 39         | 6-Hydroxy-7-methoxyflavone                              | 88         | 7-Hydroxy-4-methyl-8-nitrocoumarin                           |
| 40         | 7-Hydroxy-4'-methoxyflavone                             | 89         | 7-Hydroxy-3(4'-methoxy phenyl)-coumarin                      |
| 41         | 3-Hydroxy-7,3',4',5'-tetramethoxyflavone                | 90         | 6-Methoxy-3-phenyl-coumarin                                  |
| 42         | 3-Hydroxy-3',4',5'-trimethoxyflavone                    | 91         | 7-Methoxy-3-phenyl-coumarin                                  |
| 43         | 3,4'-Dimethoxy-2'-Hydroxychalcone                       | 92         | 7,8-Dihydroxy-coumarin                                       |
| 44         | 3',4'-Dimethoxy-2'-hydroxychalcone                      | 93         | 6-Hydroxy-7-methoxy-4-phenyl-coumarin                        |
| 45         | 4,4'-Dimethoxy-2'-hydroxychalcone                       | 94         | 7-Amino-2-methyl-chromone                                    |
| 46         | 2,4-Dimethoxy-2'-hydroxy-5'-methylchalcone              | 95         | 4,5,7-Trihydroxy-3-phenyl-coumarin                           |
| 47         | 2,5-Dimethoxy-2'-hydroxy-5-methylchalcone               | 96         | 2-Amino-7-hydroxy-4-pyridin-4-yl-4H-chromene-3-carbonitrile  |
| 48         | 5,6,7-Trihydroxyflavone                                 | 97         | 3-Phenoxy-7,8-dihydroxy-4H-chromene-4-one                    |
| 49         | 7,8,3'-Trihydroxyflavone                                | 99         | 7-Methoxy-2,8-dimethyl-3-(4-nitro-phenoxy)-chromen-4-one     |
| 50         | 7,8,4'-Trihydroxyflavone                                | 100        | 6,7-Dimethoxy-2-phenylquinoxaline                            |
| 51         | 7,8,3',4'-Tetrahydroxyflavone                           |            |  |

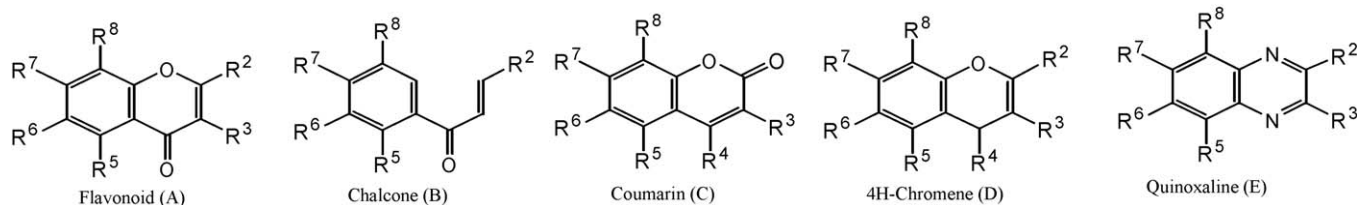
topography is such that an activity enhancing interaction at the binding domain of the 2-position phenyl ring (possibly a hydrogen bonding interaction) requires a consecutive shift of the hydroxyl substituent from the 2'- through the 4'-position to take advantage of it in going from hCNT1 through hCNT3, respectively. Although the presence of 7,8-dihydroxyl substitution generally enhances potency, this was not the case with compound **36**, in which an additional 3,5-dihydroxyl substitution appears to exert a detrimental effect that outweighed the favorable contribution of the 7,8-dihydroxyl feature. Glycosylation of the 8-position OH in the flavones was detrimental to activity (compounds **37** and **73**). However, since only one position was glycosylated it cannot be generalized that glycosylation is not tolerated. In the case of phloridzin as well as other dihydrochalcones and chalcones we previously studied, deglycosylation reduces activity; but at the same time the position of the glycosyl group was important [26].

The fact that compound **89** was potent against hCNT1 whereas closely related coumarin derivatives such as compounds **90** and **91** were not, suggests that hydrogen bonding interaction at the coumarin 7-position may contribute importantly to binding at the hCNT1 transporter. However, interactions other than those

involving the coumarin 7-position OH also contributed to the SAR of the coumarins since compounds **88**, **92** and **95** all have a free 7-OH substituent but were inactive. The presence of additional substituents that are absent in compound **89** might have caused unfavorable steric and/or electrostatic interactions at the coumarin-binding site on hCNT1. Apart from the coumarin scaffold, another structural determinant of selectivity towards hCNT1 relative to hCNT2 is the presence of 6,7-dihydroxyl substitution (compound **48**). Methylation of the hydroxyl groups is detrimental to inhibitory activity particularly against hCNT1 and hCNT2, which suggests the possible involvement of hydrogen bond donor interactions at the binding sites, but the loss of activity, could also be due to steric hindrance. The former possibility is consistent with the fact that hydrogen bond donor interactions were found to be more important relative to hydrogen bond acceptor interactions. Isoflavones were less potent than the corresponding flavones, and were generally selective towards hCNT3. Interestingly, replacing the 3-position phenyl group of isoflavones with a 4-methyl-2-thiazolyl group dramatically improved activity towards hCNT2 and hCNT3, particularly the latter (compare compound **82** with compound **83**). Modifications at this position



**Fig. 5.** Inhibition profiles of hCNT1, hCNT2 and hCNT3 by benzopyranone derivatives.  $[^3\text{H}]$ uridine uptake ( $0.2\ \mu\text{M}$ ; 2 min) was measured in PK15hCNT1, PK15hCNT2 or PK15hCNT3 cells in the absence (control) or presence of  $10\ \mu\text{M}$  of test compound incubated with cells for 15 min prior to addition of  $[^3\text{H}]$ uridine. Data points are the mean  $\pm$  S.E.M. ( $n = 3$ ).

**Table 2**Structures hCNT3 transporter inhibitory activities of compounds tested for hCNT1, hCNT2 and with IC<sub>50</sub> values where determined.

| Compound   | Type | R <sup>2</sup>                | R <sup>3</sup>   | R <sup>4</sup> | R <sup>5</sup>   | R <sup>6</sup>   | R <sup>7</sup>   | R <sup>8</sup>    | hCNT1 IC <sub>50</sub> (μM) <sup>a</sup> | hCNT2 IC <sub>50</sub> (μM) | hCNT3 IC <sub>50</sub> (μM) |
|------------|------|-------------------------------|------------------|----------------|------------------|------------------|------------------|-------------------|--|-----------------------------|-----------------------------|
| Phloridzin |      |                               |                  |                |                  |                  |                  |                   | 247.30 ± 2.10                            | 121.00 ± 1.70               | 25.13 ± 3.75                |
| 1          | A    | 4-Bromophenyl                 | H                | C=O            | H                | Cl               | CH <sub>3</sub>  | H                 | –  | –                           | –                           |
| 2          | A    | 4-Hydroxyphenyl               | OH               | C=O            | H                | H                | H                | H                 | –  | –                           | 55.68 ± 4.50                |
| 3          | A    | 3,4-Dihydroxyphenyl           | H                | C=O            | H                | H                | OH               | H                 | –  | 28.84 ± 1.40                | 11.29 ± 3.79                |
| 4          | A    | Phenyl                        | OH               | C=O            | OH               | H                | H                | H                 | –  | –                           | 34.36 ± 1.00                |
| 5          | A    | Phenyl                        | OH               | C=O            | H                | OH               | H                | H                 | –  | –                           | 11.00 ± 3.57                |
| 6          | A    | Phenyl                        | OH               | C=O            | H                | H                | OH               | H                 | –  | –                           | 104.07 ± 26.81              |
| 8          | A    | 4-Hydroxyphenyl               | H                | C=O            | H                | OH               | H                | H                 | –  | –                           | 22.26 ± 5.98                |
| 9          | A    | Phenyl                        | H                | C=O            | H                | OH               | OH               | H                 | 30.67 ± 1.40                             | 40.43 ± 1.50                | 71.74 ± 5.83                |
| 10         | A    | 2-Hydroxyphenyl               | H                | C=O            | H                | H                | OH               | H                 | –  | –                           | 18.07 ± 4.02                |
| 11         | A    | 3-Hydroxyphenyl               | H                | C=O            | H                | H                | OH               | H                 | 41.69 ± 1.50                             | 13.80 ± 1.40                | 8.86 ± 3.78                 |
| 12         | A    | 4-Hydroxyphenyl               | H                | C=O            | H                | H                | OH               | H                 | 35.75 ± 1.70                             | 24.40 ± 1.30                | 4.74 ± 1.13                 |
| 13         | A    | Phenyl                        | H                | C=O            | H                | H                | OH               | OH                | 40.43 ± 1.80                             | 3.38 ± 1.10                 | 1.62 ± 0.81                 |
| 14         | A    | 4-Hydroxyphenyl               | H                | C=O            | OH               | H                | OCH <sub>3</sub> | H                 | –  | –                           | 74.00 ± 6.85                |
| 15         | A    | Phenyl                        | H                | C=O            | OH               | OH               | OCH <sub>3</sub> | H                 | –  | 100.00 ± 1.70               | 26.26 ± 3.60                |
| 16         | A    | 3,4,5-Trimethoxyphenyl        | OH               | C=O            | H                | H                | OH               | H                 | –  | 43.10 ± 1.20                | 34.34 ± 2.79                |
| 17         | A    | 3-Hydroxy-4-methoxyphenyl     | H                | C=O            | OH               | OCH <sub>3</sub> | OCH <sub>3</sub> | H                 | –  | –                           | 17.15 ± 1.61                |
| 18         | A    | 2,3-Dimethoxyphenyl           | H                | C=O            | H                | H                | H                | H                 | –  | –                           | –                           |
| 19         | A    | 4-Methoxyphenyl               | OCH <sub>3</sub> | C=O            | H                | H                | H                | H                 | –  | –                           | 64.60 ± 2.61                |
| 20         | A    | 3,4-Dimethoxyphenyl           | H                | C=O            | H                | H                | H                | H                 | –  | –                           | –                           |
| 22         | A    | Phenyl                        | H                | C=O            | H                | OCH <sub>3</sub> | OCH <sub>3</sub> | H                 | –  | –                           | 176.73 ± 20.97              |
| 23         | A    | 3,4-Dimethoxyphenyl           | OH               | C=O            | H                | H                | H                | H                 | –  | –                           | 18.07 ± 4.02                |
| 24         | A    | 2,3-Dimethoxyphenyl           | OH               | C=O            | H                | H                | H                | H                 | –  | –                           | –                           |
| 25         | A    | 2,4-Dimethoxyphenyl           | H                | C=O            | H                | H                | H                | H                 | –  | –                           | –                           |
| 26         | A    | 2-Methoxyphenyl               | OH               | C=O            | H                | OCH <sub>3</sub> | H                | H                 | –  | –                           | –                           |
| 27         | A    | 3-Methoxyphenyl               | OH               | C=O            | H                | OCH <sub>3</sub> | H                | H                 | –  | –                           | 22.92 ± 7.02                |
| 28         | A    | 4-Methoxyphenyl               | OH               | C=O            | H                | OCH <sub>3</sub> | H                | H                 | –  | –                           | –                           |
| 30         | A    | 3-Methoxyphenyl               | OH               | C=O            | H                | H                | OCH <sub>3</sub> | H                 | –  | –                           | 56.25 ± 8.47                |
| 31         | A    | 2,4-Dimethoxyphenyl           | OH               | C=O            | H                | CH <sub>3</sub>  | H                | H                 | –  | –                           | 28.15 ± 5.75                |
| 32         | A    | 3,4-Dimethoxyphenyl           | OH               | C=O            | H                | CH <sub>3</sub>  | H                | H                 | –  | –                           | 32.08 ± 4.49                |
| 33         | A    | 3,4-Dimethoxyphenyl           | H                | C=O            | OH               | OCH <sub>3</sub> | OCH <sub>3</sub> | H                 | –  | –                           | 16.16 ± 3.06                |
| 34         | A    | 3,4-Dihydroxyphenyl           | OH               | C=O            | H                | H                | OH               | H                 | 26.30 ± 1.20                             | 8.80 ± 1.20                 | 4.25 ± 0.53                 |
| 35         | A    | 3,4,5-Trimethoxyphenyl        | H                | C=O            | OH               | OCH <sub>3</sub> | OCH <sub>3</sub> | OCH <sub>3</sub>  | –  | –                           | 49.83 ± 7.98                |
| 36         | A    | 3,4-Dihydroxyphenyl           | OH               | C=O            | OH               | H                | OH               | OH                | –  | –                           | –                           |
| 37         | A    | 3,4-Dihydroxyphenyl           | OH               | C=O            | OH               | H                | OH               | OGLu <sup>b</sup> | –  | –                           | –                           |
| 38         | A    | 3,4,5-Trimethoxyphenyl        | H                | C=O            | OCH <sub>3</sub> | OCH <sub>3</sub> | OCH <sub>3</sub> | H                 | –  | –                           | –                           |
| 39         | A    | Phenyl                        | H                | C=O            | H                | OH               | OCH <sub>3</sub> | H                 | –  | –                           | 0.57 ± 0.20                 |
| 40         | A    | 4-Methoxyphenyl               | H                | C=O            | H                | H                | OH               | H                 | –  | –                           | 27.18 ± 7.25                |
| 41         | A    | 3,4,5-Trimethoxyphenyl        | OH               | C=O            | H                | H                | OCH <sub>3</sub> | H                 | –  | –                           | –                           |
| 42         | A    | 3,4,5-Trimethoxyphenyl        | OH               | C=O            | H                | H                | H                | H                 | –  | –                           | 18.04 ± 2.71                |
| 43         | B    | 2-Hydroxy-4-methoxyphenyl     | H                | C=O            | H                | OCH <sub>3</sub> | H                | H                 | –  | –                           | 23.34 ± 5.57                |
| 44         | B    | 3,4-Dimethoxy-2-hydroxyphenyl | H                | C=O            | H                | H                | H                | H                 | –  | –                           | 24.27 ± 3.08                |
| 45         | B    | 2-Hydroxy-4-methoxyphenyl     | H                | C=O            | H                | H                | OCH <sub>3</sub> | H                 | –  | –                           | 44.14 ± 8.10                |
| 46         | B    | 2-Hydroxy-5-methylphenyl      | H                | C=O            | OCH <sub>3</sub> | H                | OCH <sub>3</sub> | H                 | –  | –                           | 43.44 ± 9.60                |
| 47         | B    | 2-Hydroxy-5-methylphenyl      | H                | C=O            | OCH <sub>3</sub> | H                | H                | OCH <sub>3</sub>  | –  | –                           | 51.44 ± 4.26                |



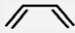

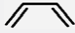

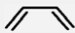
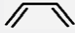

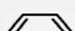

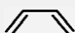

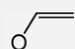
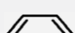
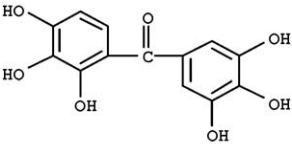
|                 |   |                        |                                  |     |  |    |   |                   |                |               |               |
|-----------------|---|------------------------|----------------------------------|-----|--|----|---|-------------------|----------------|---------------|---------------|
| 48              | A | Phenyl                 | H                                | C=O | OH   | OH | OH  | H                 | 23.99 ± 2.30   | 67.22 ± 1.60  | 29.83 ± 11.98 |
| 49              | A | 3-Hydroxyphenyl        | H                                | C=O | H  | H  | OH  | OH                | 11.75 ± 1.50   | 1.66 ± 1.10   | 7.18 ± 1.76   |
| 50              | A | 4-Hydroxyphenyl        | H                                | C=O | H  | H  | OH  | OH                | 29.39 ± 1.80   | 5.25 ± 1.20   | 0.68 ± 0.23   |
| 51              | A | 3,4-Dihydroxyphenyl    | H                                | C=O | H  | H  | OH  | OH                | 25.51 ± 1.70   | 5.62 ± 1.10   | 8.45 ± 0.22   |
| 52              | A | Phenyl                 | H                                | C=O | OH   | OH | H   | H                 | –              | –             | 15.77 ± 3.60  |
| 53              | A | 3-Hydroxyphenyl        | H                                | C=O | H  | H  | OH  | H                 | –              | 122.10 ± 9.80 | –             |
| 54              | A | 3,4-Dihydroxyphenyl    | H                                | C=O | H  | H  |    |                   | 231.74 ± 1.90  | 11.20 ± 1.50  | 32.50 ± 9.66  |
| 55              | A | Phenyl                 | H                                | C=O | H  | H  | OCH <sub>3</sub>  | OCH <sub>3</sub>  | –              | –             | 25.90 ± 3.96  |
| 56              | A | Phenyl                 | H                                | C=O | H  | H  | OCH <sub>3</sub>  | OH                | –              | –             | 35.55 ± 2.90  |
| 57              | A | 2-Hydroxyphenyl        | H                                | C=O | H  | H  | OH  | OH                | 16.60 ± 1.50   | 4.06 ± 1.30   | 9.51 ± 1.67   |
| 58              | A | H                      | 4-Chloro phenyl                  | C=O | H  | H  | OH  | CH <sub>3</sub>   | –              | –             | 43.63 ± 10.1  |
| 59              | A | H                      | Phenyl                           | C=O | H  | H  | OH  | –                 | –              | –             | 31.62 ± 7.68  |
| 60              | A | Phenyl                 | H                                | C=O |   |    | H   | H                 | –              | –             | 20.33 ± 3.53  |
| 61              | A | Phenyl                 | H                                | C=O | H  | H  |    |                   | –              | –             | 32.36 ± 0.42  |
| 62              | A | 3,4-Dihydroxyphenyl    | H                                | C=O |   |    | H   | H                 | –              | –             | 13.48 ± 2.47  |
| 63              | A | 3,4-Dimethoxyphenyl    | H                                | C=O | H  | H  |    |                   | –              | –             | 14.69 ± 8.00  |
| 64              | A | 2-Hydroxyphenyl        | H                                | C=O | H  | H  |    |                   | –              | –             | 30.47 ± 5.10  |
| 65              | A | 2-Hydroxyphenyl        | H                                | C=O |   |    | H   | H                 | –              | –             | 32.95 ± 5.99  |
| 66              | A | 3-Hydroxyphenyl        | H                                | C=O | H  | H  |    |                   | –              | –             | 16.39 ± 7.56  |
| 67              | A | 3-Hydroxyphenyl        | H                                | C=O |   |    | H   | H                 | –              | –             | 16.96 ± 7.07  |
| 68              | A | 4-Hydroxyphenyl        | H                                | C=O | H  | H  |    |                   | –              | –             | 39.51 ± 1.06  |
| 69              | A | 4-Hydroxyphenyl        | H                                | C=O |  |    | H   | H                 | –              | –             | 42.00 ± 3.31  |
| 70              | A | Phenyl                 | OCH <sub>3</sub>                 | C=O | H  | H  |  |                   | –              | –             | 20.21 ± 6.90  |
| 71              | A | 4-Methoxyphenyl        | H                                | C=O | H  | H  |  |                   | –              | –             | 15.87 ± 4.85  |
| 72              | A | 3,4,5-Trihydroxyphenyl | H                                | C=O | OH   | H  | OH  | H                 | 24.73 ± 1.20   | 15.80 ± 1.40  | 6.59 ± 1.17   |
| 73              | A | 4-Hydroxyphenyl        | H                                | C=O | H  | H  | OH  | OGlu <sup>b</sup> | – <sup>c</sup> | –             | 26.97 ± 4.74  |
| 74              | A | H                      | (1-Phenyl-1H-pyrazol-4-yl)       | C=O | H  | H  | OH  | OH                | 27.90 ± 1.80   | 79.43 ± 3.10  | 7.42 ± 1.66   |
| 75              | A | Phenyl                 | H                                | C=O | H  | H  | H   | H                 | –              | –             | 26.06 ± 5.48  |
| 77              | A | Phenyl                 | H                                | C=O | H  | Cl | Cl  | H                 | –              | –             | 34.68 ± 8.56  |
| 78              | A | H                      | 4-Chloro phenoxy                 | C=O | H  | H  | OH  | OH                | –              | –             | 31.71 ± 5.70  |
| 79              | A | H                      | 4-Fluoro phenoxy                 | C=O | H  | H  | OH  | OH                | –              | –             | 27.06 ± 1.28  |
| 80              | A | Methyl                 | Phenyl                           | C=O | H  | H  | OH  | OH                | –              | –             | 22.93 ± 1.46  |
| 81              | A | H                      | Phenyl                           | C=O | H  | OH | OH  | H                 | 34.62 ± 2.10   | 141.00 ± 2.40 | 26.25 ± 4.47  |
| 82              | A | H                      | Phenyl                           | C=O | H  | H  | OH  | OH                | 98.23 ± 2.70   | 126 ± 1.90    | 55.83 ± 11.99 |
| 83              | A | H                      | (4-CH <sub>3</sub> -2-thiazolyl) | C=O | H  | H  | OH  | OH                | 51.88 ± 1.90   | 20.00 ± 1.60  | 3.02 ± 1.95   |
| 84              | A | 3,4,5-Trihydroxyphenyl | OH                               | C=O | H  | H  | OH  | H                 | 27.12 ± 2.10   | 13.30 ± 1.30  | 1.04 ± 0.60   |
| 85              | A | 3,4,5-Trihydroxyphenyl | H                                | C=O | H  | H  | OH  | H                 | 23.99 ± 1.60   | 8.17 ± 1.20   | 12.05 ± 1.17  |
| 86 <sup>d</sup> |   |                        |                                  |     |  |    |   |                   | –              | –             | –             |
| 87 <sup>e</sup> |   |                        |                                  |     |  |    |   |                   | –              | –             | –             |

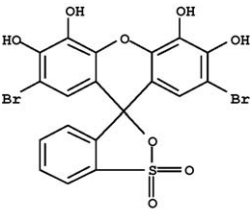
Table 2 (Continued)

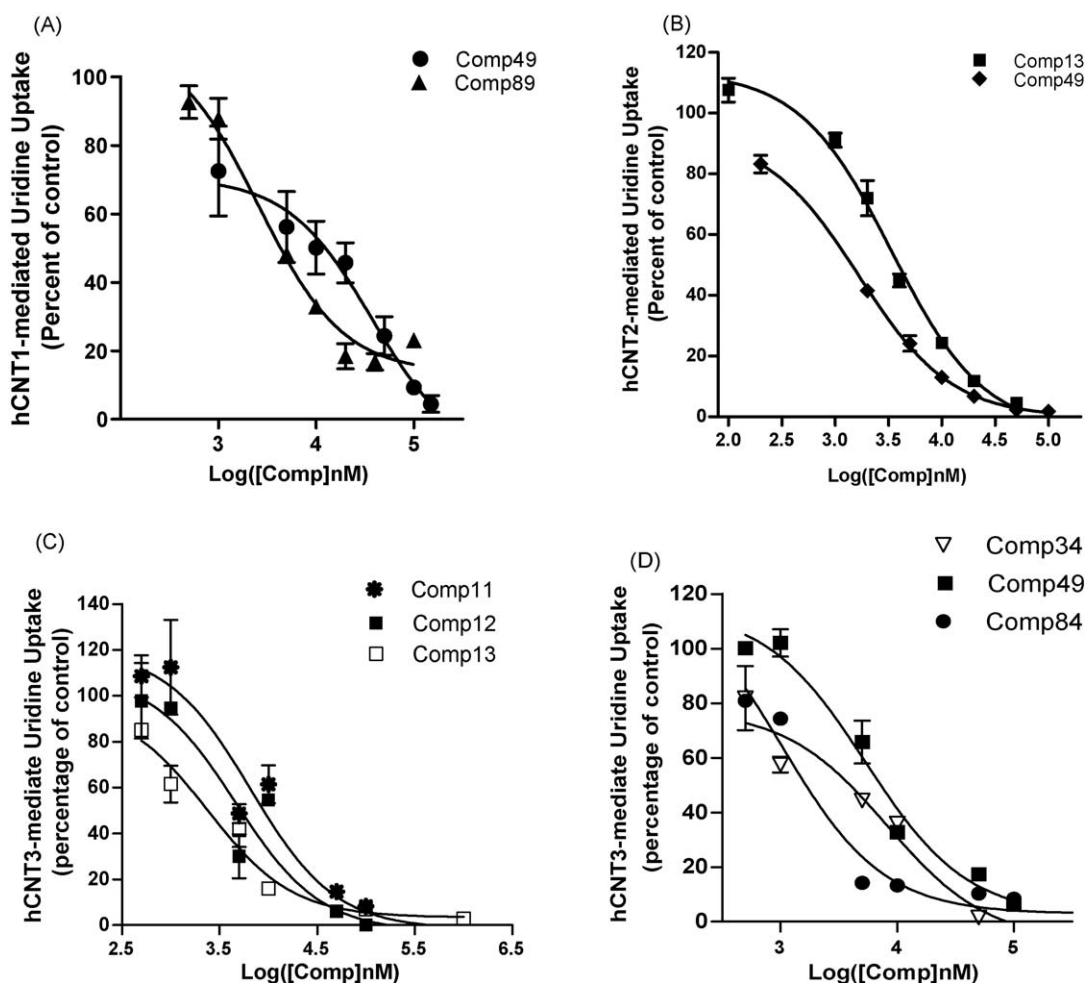
| Compound | Type | R <sup>2</sup>  | R <sup>3</sup>         | R <sup>4</sup>  | R <sup>5</sup> | R <sup>6</sup>   | R <sup>7</sup>   | R <sup>8</sup>  | hCNT1 IC <sub>50</sub> (μM) <sup>a</sup> | hCNT2 IC <sub>50</sub> (μM) | hCNT3 IC <sub>50</sub> (μM) |
|----------|------|-----------------|------------------------|-----------------|----------------|------------------|------------------|-----------------|--|-----------------------------|-----------------------------|
| 88       | C    | C=O             | H                      | CH <sub>3</sub> | H              | H                | OH               | NO <sub>2</sub> | –  | –                           | –                           |
| 89       | C    | C=O             | 4'-Methoxy phenyl      | H               | H              | H                | OH               | H               | 4.44 ± 1.30                              | –                           | –                           |
| 90       | C    | C=O             | Phenyl                 | H               | H              | OCH <sub>3</sub> | H                | H               | –  | –                           | –                           |
| 91       | C    | C=O             | Phenyl                 | H               | H              | H                | OCH <sub>3</sub> | H               | –  | –                           | –                           |
| 92       | C    | C=O             | H                      | H               | H              | OH               | OH               | OH              | –  | –                           | –                           |
| 93       | C    | C=O             | H                      | phenyl          | H              | OH               | OCH <sub>3</sub> | H               | –  | –                           | –                           |
| 94       | D    | Methyl          | H                      | H               | H              | H                | NH <sub>2</sub>  | H               | –  | –                           | –                           |
| 95       | C    | C=O             | Phenyl                 | OH              | OH             | H                | OH               | H               | –  | –                           | –                           |
| 96       | D    | NH <sub>2</sub> | CN                     | Pyridin -4-yl   | H              | H                | OH               | H               | –  | –                           | 54.65 ± 2.03                |
| 97       | D    | H               | Phenoxy                | H               | H              | H                | OH               | OH              | –  | –                           | –                           |
| 99       | D    | Methyl          | 4'-Nitrophenyl phenoxy | H               | H              | H                | OCH <sub>3</sub> | CH <sub>3</sub> | –  | –                           | –                           |
| 100      | E    | Phenyl          | H                      | N               | H              | OCH <sub>3</sub> | OCH <sub>3</sub> | H               | –  | –                           | –                           |

<sup>a</sup> The uptake of 0.2 μM [<sup>3</sup>H]Uridine into PK15 cells expressing hCNT1, hCNT2 and hCNT3 was measured over 2 min in the presence of graded concentrations of benzopyrone analogs. The concentration of test compounds that caused 50% inhibition of [<sup>3</sup>H]uridine uptake (IC<sub>50</sub>, mean ± S.D., n = 3) were calculated using a nonlinear fitting method in Prism version 4.0 software (GraphPad Inc., San Diego, CA).  
<sup>b</sup> Glu: glucosyl group.  
<sup>c</sup> A dash means not determined because compound had no significant inhibitory activity.  
<sup>d</sup> Compound 86 (2,3,4,3',4',5'-hexahydroxybenzophenone).



<sup>e</sup> Compound 87 (Bromopyrogallol red).





**Fig. 6.** Concentration-dependent inhibition of hCNT1 (A), hCNT2 (B) and/or hCNT3 (C) uridine transport by the most potent benzopyranone derivatives. Graded concentrations of test compounds were incubated with cells for 15 min prior to addition of [ $^3$ H]uridine for an uptake period of 2 min. Data are presented as percent inhibition relative to vehicle control (mean  $\pm$  S.E.M.;  $n = 3$ ). Compounds shown are the ones with  $IC_{50}$ s  $\leq 5 \mu M$  for the particular hCNT.

with heterocyclic groups with hydrophilic character may lead to more potent isoflavone CNT inhibitors.

Taken together, the SARs show commonalities of some structural elements among all three hCNT transporter flavone-binding sites such as OH substitution at the 7- and 8-positions, as well as marked differences which are more clearly illustrated in the CoMFA and CoMSIA 3D-QSAR models discussed in the next section. It is clear that whereas the flavone-binding sites of hCNT1 and hCNT2 are quite stringent, that of hCNT3 is quite tolerant, thus accommodating even naphthoflavones and related compounds. The higher sensitivity of hCNT3 to the flavonoids and related compounds reflects the promiscuous substrate specificity of this transporter relative to the other CNTs. As already mentioned, hCNT3 does not discriminate between purine and pyrimidine nucleosides. hCNT3 also has other characteristics not shared by the other two hCNTs, such as Na $^{+}$ -nucleoside coupling stoichiometry of 2:1 and the ability to transport nucleosides using a H $^{+}$  gradient [15,31].

### 3.5. CoMFA and CoMSIA 3D-QSAR models

To rationalize the SAR data to obtain insights into pharmacophoric elements for transporter affinity and selectivity, as well as establish quantitative models for prediction of activity, we applied 3D-QSAR analyses to the test results. The CoMFA 3D-QSAR method introduced by Cramer et al. [23] has been used extensively and

shown to be useful for drug design. CoMSIA 3D-QSAR [24] is a related QSAR method that is increasingly being used to complement CoMFA analysis. CoMFA and CoMSIA and CoMSIA 3D-QSAR analyses have actually been recently applied to nucleoside substrates and inhibitors of ENT and CNT transporters [32,33] to explain steric, electrostatic and hydrogen bonding contributions to transporter–ligand interactions. Thus, we thought these methods would help throw more light on the intermolecular forces influencing the SAR of flavones as hCNT inhibitors.

The PLS regression analyses statistics for CoMFA and CoMSIA models established are presented in Table 3, and the results of additional validation exercises that tested robustness are presented in Table 4. The respective CoMFA and CoMSIA correlation coefficient ( $r^2$ ) values were 0.984 and 0.997 for hCNT1; 0.840 and 0.863 for hCNT2; and 0.910 and 0.919 for hCNT3. The corresponding leave-one-out cross-validated coefficient ( $q^2$ ) values were 0.525 and 0.547 for hCNT1, 0.583 and 0.613 for hCNT2, and 0.517 and 0.493 for hCNT3. The  $q^2$  values indicate that the models had fairly good predictive abilities. The results of group cross-validation, activity randomization (scrambling) and bootstrapping exercises presented in Table 4 show that the models were quite robust and not the products of chance correlation. The descriptor contributions shown in Table 3 indicate that electrostatic and hydrophobic effects were the main determinants of interactions with hCNT1, while electrostatics and hydrogen bond donor interactions dominated for hCNT2 and hCNT3. Interestingly, the

**Table 3**  
PLS statistics of CoMFA and CoMSIA 3D-QSAR models.

| PLS statistics                          | hCNT1 |        | hCNT2 |        | hCNT3 |        |
|---|-------|--------|-------|--------|-------|--------|
|   | CoMFA | CoMSIA | CoMFA | CoMSIA | CoMFA | CoMSIA |
| $q^2$ (LOO)                             | 0.525 | 0.547  | 0.583 | 0.613  | 0.517 | 0.493  |
| $r^2$                                   | 0.984 | 0.997  | 0.840 | 0.863  | 0.910 | 0.919  |
| $s$                                     | 0.037 | 0.020  | 0.247 | 0.224  | 0.141 | 0.107  |
| $F$                                     | 99.22 | 294.01 | 29.67 | 37.69  | 50.26 | 66.26  |
| PLS components                          | 5     | 6      | 3     | 3      | 7     | 6      |
| No. of compounds used for model         | 14    | 13     | 21    | 22     | 43    | 42     |
| No. of compounds in external test set   | N/A   | N/A    | N/A   | N/A    | 9     | 10     |
| Steric descriptor contribution          | 0.564 | 0.074  | 0.503 | 0.071  | 0.417 | 0.064  |
| Electrostatic descriptor contribution   | 0.436 | 0.710  | 0.497 | 0.327  | 0.583 | 0.432  |
| Hydrophobic descriptor contribution     | N/A   | 0.210  | N/A   | 0.149  | N/A   | 0.162  |
| H-bond donor descriptor contribution    | N/A   | ND     | N/A   | 0.312  | N/A   | 0.232  |
| H-bond acceptor descriptor contribution | N/A   | ND     | N/A   | 0.140  | N/A   | 0.110  |

$q^2$ : cross-validated correlation coefficient;  $s$ : standard error;  $r^2$ : non-validated correlation coefficient;  $F$ :  $F$ -test value.

**Table 4**  
Results of group cross-validation, randomization and bootstrapping for 3D-QSAR models.

| Method   | hCNT1         |               | hCNT2         |               | hCNT3         |               |
|--|---------------|---------------|---------------|---------------|---------------|---------------|
|  | CoMFA         | CoMSIA        | CoMFA         | CoMSIA        | CoMFA         | CoMSIA        |
| Group validation $q^2$ (30 groups and 30 runs) | 0.525 ± 0.030 | 0.547 ± 0.029 | 0.583 ± 0.015 | 0.623 ± 0.009 | 0.513 ± 0.023 | 0.495 ± 0.012 |
| Randomization $q^2$ (20 runs)                  | −0.371        | −0.075        | −0.150        | −0.107        | −0.005        | −0.034        |
| Bootstrapping (20 runs) 1. $r^2$               | 0.984 ± 0.007 | 0.999 ± 0.001 | 0.917 ± 0.009 | 0.920 ± 0.016 | 0.945 ± 0.028 | 0.961 ± 0.013 |
| 2. S.D.  | 0.018 ± 0.002 | 0.011 ± 0.014 | 0.040 ± 0.012 | 0.028 ± 0.005 | 0.112 ± 0.077 | 0.073 ± 0.043 |

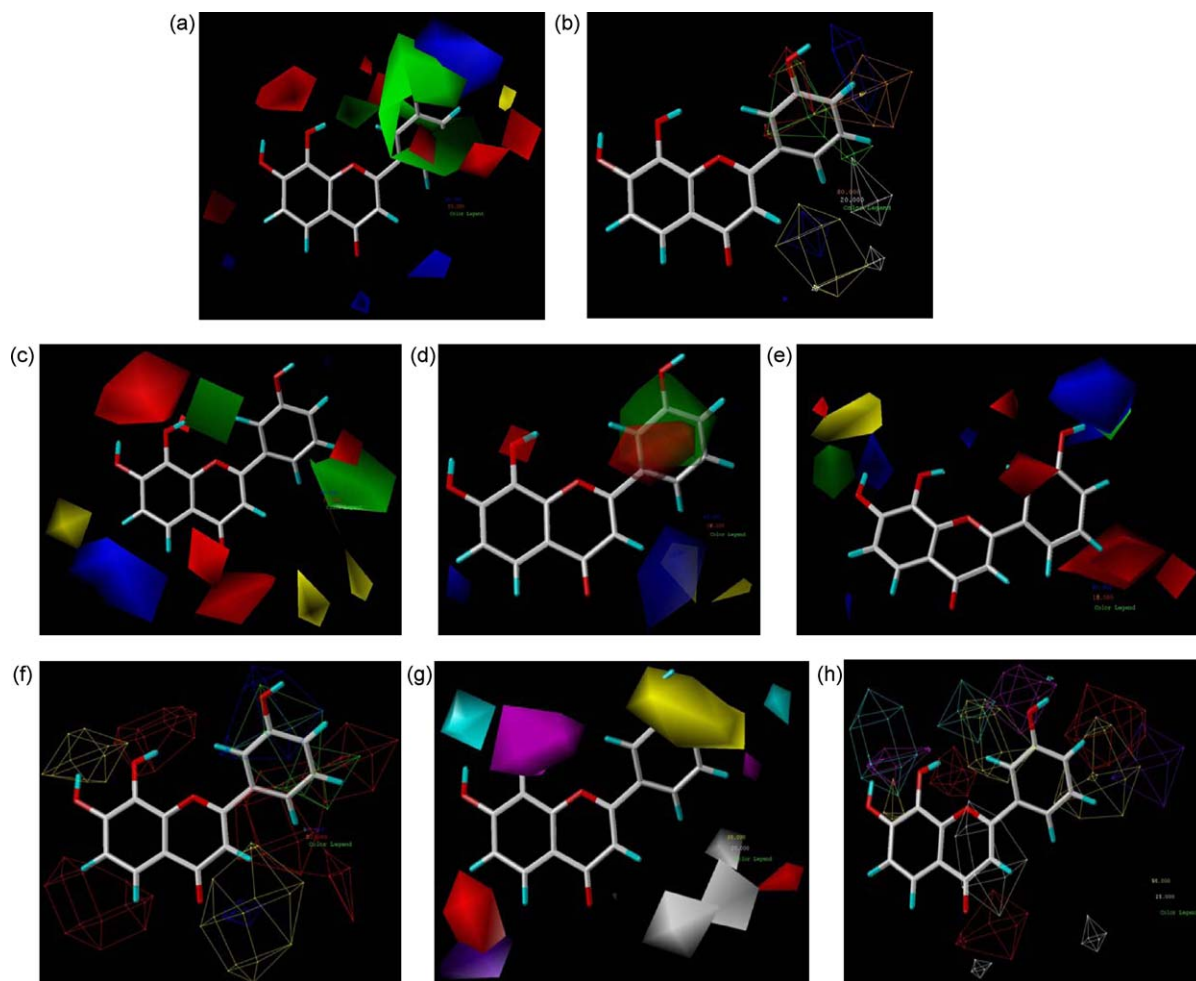
$q^2$ : cross-validated correlation coefficient;  $r^2$ : non-validated correlation coefficient, S.D.: standard deviation.

same trend of descriptor contributions was uncovered in CoMFA and CoMSIA modeling of the SARs of nucleoside analog inhibitors and substrate interactions for these transporters [32,33]. It will be interesting to find out whether any of the OH groups of these flavones interact in a similar fashion to the 3'-OH and 5'-OH groups of nucleosides that have been shown to have important hydrogen bonding interactions with hCNT1 and hCNT2.

To identify regions in 3D space where changes in the particular intermolecular interaction forces increase or decrease inhibitory activity for each transporter subtype, PLS coefficient contour maps for CoMFA and CoMSIA descriptor fields were generated and projected onto compound **49** as shown in Fig. 7. The contours generally show a similar strong preference for electronegative substituents at the 8-position (red contours, Fig. 7a, c, d and f). For hCNT1, electronegative substituents are also preferred at the 6-position and around the 2-position phenyl ring (Fig. 7a), which have similarities with the hCNT3 models (Fig. 7e and f). This suggests similarities in these binding regions of flavones at hCNT1 and hCNT3 but not at hCNT2. Other differences in electronegative substituent preferences between hCNT1/3 and hCNT2 are strong preference at the 4-position (Fig. 7c) and the core of the whole 2-position substituent for the latter transporter (Fig. 7d). With regard to electropositive substituents, hCNT1 and hCNT3 have similar strong preferences at the 3'-/4'-positions (Fig. 7a, e and f), but the two transporters differ by hCNT1 also favoring electropositive substituents at the 3- and 4-positions (Fig. 7a and b) whereas hCNT3 favors them at the 7-position (Fig. 7e), besides the common the 3'-/4'-positions. The electropositive substituent preferences of hCNT1 and hCNT2 are similar at the 3-position. In addition to favoring electropositive substituents at the 3-position, hCNT2 also has a strong electropositive substituent preference at the 5- and 6-positions (Fig. 7c and d). Although steric interactions did not significantly influence activity (see contribution from CoMSIA models, Table 3), the contours show there is a general preference for substituents with steric bulk at the 2-position (Fig. 7a–f). With hCNT3, there is additional preference of small steric bulk at the 7-position going toward the 6-position (Fig. 7e). Juxtaposed to this

region, is a yellow region showing steric restriction (Fig. 7e and f). A prominent region of the flavone template where bulk is generally not tolerated for all three transporters is the 3-position (Fig. 7b–d and f). This is reflected in the SAR by the lower activity of isoflavones (with 3-position phenyl group) relative to flavones (with 2-position phenyl group). Previous 3D-QSAR studies on hCNT1 and hCNT2 interaction with nucleosides suggested that steric and electrostatic interactions were important for affinity at hCNT1, while hydrogen bonding interactions were important for hCNT2 inhibition [32]. In the case of the flavone inhibitors, electrostatic interactions were predominant while steric effects were not very significant. Hydrophobic interactions also featured prominently in the interaction of flavones with all the transporters, particularly hCNT1 (Table 3). All three transporters favor hydrophobic substituent at the 2-position but generally disfavor hydrophobic groups at the 3-position (Fig. 7b, g and h). Hydrogen bonding interactions were not important for flavone interactions with hCNT1, but were significant for hCNT2 and hCNT3. Hydrogen bond donor effects predominated over acceptor effects, and hCNT2 was the most affected. This is interesting in light of the interaction of nucleoside inhibitors with hCNT2, where the predominance of hydrogen bond donor effects over acceptor effects was also observed [32], leading to the suggestion that the inhibitor binding site of the hCNT2 transporter may be rich in amino acids with strong hydrogen bond acceptor features. The contour maps suggest that for hCNT2, the 7-position OH group is a hydrogen bond donor whereas the 8-position OH group is an acceptor involving the oxygen atom (Fig. 7g). The 5- and 6-positions were shown to be intolerant of hydrogen bond donor or acceptor substituents with respect to hCNT2 inhibitory activity. For hCNT3, both the 7- and 8-position OH groups are suggested to be engaged in both H-bond donor and H-bond acceptor interactions (Fig. 7h). Additionally, a hydrogen bond donor interaction is suggested for flavones at the 4'-position for hCNT2 (Fig. 7g), and an acceptor interaction is indicated at the 3'-position for hCNT3 (Fig. 7h). It is important to note that two previous reported hCNT3 3D-QSAR models of nucleoside analogs indicated that the minimal structural determinants for hCNT3 substrates were two hydrogen





**Fig. 7.** CoMFA and CoMSIA PLS field coefficient contour maps (a) CoMFA steric and electrostatic contours for hCNT1; (b) CoMSIA steric, electrostatic and hydrophobic contours for hCNT1; (c) CoMFA steric and electrostatic contours for hCNT2; (d) CoMSIA steric and electrostatic contours for hCNT2; (e) CoMFA steric and electrostatic contours for hCNT3; (f) CoMSIA steric and electrostatic contours for hCNT3; (g) CoMSIA hydrophobic, H-bond donor and acceptor contours for hCNT2; and (h) CoMSIA hydrophobic, H-bond donor and acceptor contours for hCNT3. *Color legend:* For CoMFA and CoMSIA steric and electrostatic contours (a, c, e, f and g), green and yellow contours, depict sterically favored and disfavored regions, respectively; and the blue and red contours indicate regions favoring electropositive and electronegative substituents, respectively. For CoMSIA steric, electrostatic and hydrophobic contours for hCNT1 (b), green and yellow contours, depict sterically favored and disfavored regions, respectively; the blue and red contours indicate regions favoring electropositive and electronegative substituents, respectively; and orange and white contours denote regions that favor or disfavor hydrophobic groups, respectively. For CoMSIA hydrophobic and hydrogen bonding contours for hCNT2 and hCNT3, (g and h), yellow and white contours denote regions that favor or disfavor hydrophobic groups, respectively; cyan and purple contours indicate regions that favor or disfavor H-bond donors, respectively; and magenta and red contours identify favorable and unfavorable regions for H-bond acceptors, respectively. Some contours are displayed as wires to allow for visualization even when contours overlap extensively.

bond acceptors at the 3'- and 5'-positions of the ribose moiety, and a hydrophobic center occupied by the base ring [33].

#### 4. Conclusion

The elucidation of the physiological roles of concentrative nucleoside transporters is still in its infancy, and several patterns are beginning to emerge pointing to functions beyond nucleoside and nucleotide salvage mechanisms, to include nucleoside reabsorption and secretion processes as well as signal transduction. Besides, the CNTs are also implicated in the absorption and efficacy of nucleoside analog anticancer and antiviral drugs. Despite the physiological and pharmacological importance of these transporters, only a very limited number of potent nucleoside-based inhibitors are known, but only limited to CNT2, including 5'-position modified nucleoside derivatives of adenosine, benzimidazole ribofuranosides and 8-position modified purine nucleoside derivatives [34–36]. Phloridzin is the standard CNT inhibitor, but has only moderate activity at best [25]. These cells and previously

established hCNT3 expressing K15NTD cells [25] were successfully used as a testing platform to discover the first potent and selective non-nucleoside CNT inhibitors. In screening of flavonoids and coumarin benzopyranone derivatives and related compounds, we have identified potent and selective inhibitors for each individual cloned hCNT, i.e. hCNT1, hCNT2 and hCNT3. 3D-QSAR modeling of the SAR data provided insights into structural determinants of flavone activity and selectivity as hCNT inhibitors. Thus, electrostatic interactions predominated for all three hCNTs; and while hydrophobic interactions were also important for all three hCNTs, hydrogen bonding interactions were not significant for the SAR of hCNT1, but featured prominently in the interactions with hCNT2 and hCNT3, particularly hydrogen bond donor interactions. These results are consistent with the observation in the SAR that the 7,8-dihydroxy-substitution is a high potency structural determinant among the flavones and isoflavones. These models provide a good starting point for lead optimization. Refinement of the QSAR models with larger sets of compounds will improve their utility as predictive tools.

Nucleoside transporter inhibitors have potential therapeutic uses in biological response modification of antimetabolite chemotherapy, in ischemic heart disease and stroke, kidney transplantation, hypertension, analgesia, inflammation [20]. CNT inhibitors have potential uses in hyperuricemia, gout and hyperuric nephropathy [35]. Nucleoside analogues are widely used for the treatment of cancers and viral infections; they can cause normal tissue toxicity resulting in serious side effects like myelosuppression and gastrointestinal toxicity. Non-nucleoside inhibitors such as the flavonoids reported here may overcome the shortcomings of nucleoside analogue inhibitors. Flavonoids occur widely in nature and are commonly found in fruits, vegetables and wine, which are components of human diet, and thought to reduce disease risks, and are thus not likely to be toxic, and have better prospects for drug development than their potentially cytotoxic nucleoside counterparts.

This study is not only important because potent and selective novel CNT inhibitors were discovered as potential pharmacological agents and/or research tools, but also because it shows that flavonoids present in foods and dietary supplements may affect the efficacy of nucleoside-derived anticancer and antiviral drugs that are substrates of CNTs such as gemcitabine [37], 5-azacytidine [38] and AZT [39]. The inhibitors identified in this study are the most potent and selective non-nucleoside hCNT inhibitors reported to date, and can serve as new lead compounds for the development of more potent and more selective hCNT inhibitors.

## Acknowledgments

We thank Dr. Chung-Ming Tse for his kind provision of PK15NTD cells and PK15/hCNT3 cells.

We also thank Dr. Parker Suttle of the Pharmacology Department for useful suggestions and assistance.

## References

- [1] Griffith DA, Jarvis SM. Nucleoside and nucleobase transport systems of mammalian cells. *Biochim Biophys Acta* 1996;1286:153–81.
- [2] King AE, Ackley MA, Cass CE, Young JD, Baldwin SA. Nucleoside transporters: from scavengers to novel therapeutic targets. *Trends Pharmacol Sci* 2006;27:416–25.
- [3] Jennings LL, Hao C, Cabrita MA, Vickers MF, Baldwin SA, Young JD, et al. Distinct regional distribution of human equilibrative nucleoside transporter proteins 1 and 2 (hENT1 and hENT2) in the central nervous system. *Neuropharmacology* 2001;40:722–31.
- [4] Latini S, Pedata F. Adenosine in the central nervous system: release mechanisms and extracellular concentrations. *J Neurochem* 2001;79:463–84.
- [5] Damaraju VL, Damaraju S, Young JD, Baldwin SA, Mackey J, Sawyer MB, et al. Nucleoside anticancer drugs: the role of nucleoside transporters in resistance to cancer chemotherapy. *Oncogene* 2003;22:7524–36.
- [6] Pastor-Anglada M, Cano-Soldado P, Molina-Arcas M, Lostao MP, Larráyoz I, Martínez-Picado J, et al. Cell entry and export of nucleoside analogues. *Virus Res* 2005;107:151–64.
- [7] Molina-Arcas M, Trigueros-Motos L, Casado FJ, Pastor-Anglada M. Physiological and pharmacological roles of nucleoside transporter proteins. *Nucleosides Nucleotides Nucleic Acids* 2008;27:769–78.
- [8] Baldwin SA, Beal PR, Yao SY, King AE, Cass CE, Young JD. The equilibrative nucleoside transporter family, SLC29. *Pflügers Arch Eur J Physiol* 2004;447:735–43.
- [9] Gray JH, Owen RP, Giacomini KM. The concentrative nucleoside transporter family, SLC28. *Pflügers Arch Eur J Physiol* 2004;447:728–34.
- [10] Huang QQ, Yao SY, Ritzel MW, Paterson AR, Cass CE, Young JD. Cloning and functional expression of a complementary DNA encoding a mammalian nucleoside transport protein. *J Biol Chem* 1994;269:17757–60.
- [11] Che M, Ortiz DF, Arias IM. Primary structure and functional expression of a cDNA encoding the bile canalicular, purine-specific Na<sup>+</sup>-nucleoside cotransporter. *J Biol Chem* 1995;270:13596–9.
- [12] Wang J, Su SF, Dresser MJ, Schaner ME, Washington CB, Giacomini KM. Na<sup>+</sup>-dependent purine nucleoside transporter from human kidney: cloning and functional characterization. *Am J Physiol* 1997;273:F1058–65.
- [13] Ritzel MW, Yao SY, Huang MY, Elliott JF, Cass CE, Young JD. Molecular cloning and functional expression of cDNAs encoding a human Na<sup>+</sup>-nucleoside cotransporter (hCNT1). *Am J Physiol* 1997;272:C707–14.
- [14] Ritzel MW, Yao SY, Ng AM, Mackey JR, Case CE, Young JD. Molecular cloning, functional expression and chromosome localization of a cDNA encoding a human Na<sup>+</sup>-nucleoside cotransporter (hCNT2) selective for purine nucleosides and uridine. *Mol Membr Biol* 1998;15:203–11.
- [15] Ritzel MW, Ng AM, Yao SY, Graham K, Leowen SK, Smith KM, et al. Molecular identification and characterization of novel human and mouse concentrative Na<sup>+</sup>-nucleoside cotransporter (hCNT3 and mCNT3) broadly selective for purine and pyrimidine nucleoside (system cib). *J Biol Chem* 2001;276:2914–27.
- [16] Yao SY, Ng AM, Slugoski MD, Smith KM, Mulinta R, Karpinski E, et al. Conserved glutamate residues are critically involved in Na<sup>+</sup>/nucleoside cotransport by human concentrative nucleoside transporter 1 (hCNT1). *J Biol Chem* 2007;282:30607–1.
- [17] Damaraju VL, Elwi AN, Hunter C, Carpenter P, Santos C, Barron GM, et al. Localization of broadly selective equilibrative and concentrative nucleoside transporters, hENT1 and hCNT3, in human kidney. *Am J Physiol Renal Physiol* 2007;293:F200–11.
- [18] Pastor-Anglada M, Cano-Soldado P, Errasti-Murugarren E, Casado FJ. SLC28 genes and concentrative nucleoside transporter (CNT) proteins. *Xenobiotica* 2008;38:972–94.
- [19] Pastor-Anglada M, Errasti-Murugarren E, Aymerich I, Casado FJ. Concentrative nucleoside transporters (CNTs) in epithelia: from absorption to cell signaling. *J Physiol Biochem* 2007;63:97–110.
- [20] Buolamwini JK. Nucleoside transporter inhibitors: structure–activity relationships and potential therapeutic applications. *Curr Med Chem* 1997;4:35–66.
- [21] Kwon O, Eck P, Chen S, Corpe CP, Lee JH, Kruhlak M, et al. Inhibition of the intestinal glucose transporter GLUT2 by flavonoids. *FASEB J* 2007;21:366–77.
- [22] Ward JL, Sherali A, Mo ZP, Tse CM. Kinetic and pharmacological properties of cloned human equilibrative nucleoside transporters, ENT1 and ENT2, stably expressed in nucleoside transporter-deficient PK15 cells. ENT2 exhibits a low affinity for guanosine and cytidine but a high affinity for inosine. *J Biol Chem* 2000;275:8375–81.
- [23] Cramer III RD, Patterson DE, Bunce JD. comparative molecular field analysis (CoMFA). 1. Effect of shape on binding of steroids to carrier proteins. *J Am Chem Soc* 1988;110:5959–67.
- [24] Klebe G, Abraham U, Mietzner T. Molecular similarity indices in a comparative analysis (CoMSIA) of drug molecules to correlate and predict their biological activity. *J Med Chem* 1994;37:4130–46.
- [25] Toan S, To KK, Leung GP, Souza MO, Ward JL, Tse C. Genomic organization and functional characterization of the human concentrative nucleoside transporter-3 isoform (hCNT3) expressed in mammalian cells. *Eur J Physiol* 2003;447:195–204.
- [26] Gupta A, Buolamwini JK. Synthesis and biological evaluation of Phloridzin analogs as human concentrative nucleoside transporter 3 (hCNT3) inhibitors. *Bioorg Med Chem Lett* 2009;19:917–21.
- [27] Smith KM, Ng AM, Yao SY, Labedz KA, Knaus EE, Wiebe LI, et al. Electrophysiological characterization of a recombinant human Na<sup>+</sup>-coupled nucleoside transporter (hCNT1) produced in *Xenopus* oocytes. *J Physiol* 2004;558:807–23.
- [28] Zhang J, Smith KM, Tackaberry T, Visser F, Robins MJ, Nielsen LP, et al. Uridine binding and transportability determinants of human concentrative nucleoside transporters. *Mol Pharmacol* 2005;68:830–9.
- [29] Lang TT, Young JD, Cass CE. Interactions of nucleoside analogs, caffeine, and nicotine with human-concentrative nucleoside transporters 1 and 2 stably produced in a transport-defective human cell line. *Mol Pharmacol* 2004;65:925–33.
- [30] Visser F, Zhang J, Raborn RT, Baldwin SA, Young JD, Cass CE. Residue 33 of human equilibrative nucleoside transporter 2 is a functionally important component of both the dipyridamole and nucleoside-binding sites. *Mol Pharmacol* 2005;67:1291–8.
- [31] Smith KM, Slugoski MD, Loewen SK, Ng AM, Yao SY, Chang XZ, et al. The broadly selective human Na<sup>+</sup>/nucleoside cotransporter (hCNT3) exhibits novel cation-coupled nucleoside transport characteristics. *J Biol Chem* 2005;280:25436–49.
- [32] Chang C, Swaan PW, Ngo LY, Lum PY, Patil SD, Unadkat JD. Molecular requirements of the human nucleoside transporters hCNT1, hCNT2, and hCNT3. *Mol Pharmacol* 2004;65:558–70.
- [33] Hu H, Endres CJ, Chang C, Umapathy NS, Lee EW, Fei YJ, et al. Electrophysiological characterization and modeling of the structure activity relationship of the human concentrative nucleoside transporter 3 (hCNT3). *Mol Pharmacol* 2006;69:1542–53.
- [34] Nonaka Y, Tatani K, Hiratochi M, Kuramochi Y, Isaji M. Preparation of 5'-modified nucleoside derivatives as CNT-2 inhibitors. *WO 2004101593*; 2004.
- [35] Kikuchi N, Nonaka Y, Tatani K, Hiratochi M, Kuramochi Y, Isaji M, et al. Preparation of ribofuranoside compounds having benzimidazole moiety as CNT2 inhibitors. *PCT Int Appl* 2005;141.
- [36] Tatani, K.N.Y., Kikuchi, N. Preparation of purine nucleoside derivatives modified in 8-position as inhibitors of concentrative nucleoside transporter 2. *WO 2006030803*; 2006.
- [37] Mackey JR, Yao SY, Smith KM, Karpinski E, Baldwin SA, Cass CE, et al. Gemcitabine transport in *xenopus* oocytes expressing recombinant plasma membrane mammalian nucleoside transporters. *J Natl Cancer Inst* 1999;91:1876–81.
- [38] Rius M, Stresemann C, Keller D, Brom M, Schirmacher E, Keppler D, et al. Human concentrative nucleoside transporter 1-mediated uptake of 5-azacytidine enhances DNA demethylation. *Mol Cancer Ther* 2009;8:225–31.
- [39] Errasti-Murugarren E, Pastor-Anglada M, Casado FJ. Role of CNT3 in the transepithelial flux of nucleosides and nucleoside-derived drugs. *J Physiol* 2007;582:1249–60.